Published online 12 December 2018

Nucleic Acids Research, 2019, Vol. 47, No. 5 ***2533–2545***
doi: 10.1093/nar/gky1250

Transfer RNA demethylase ALKBH3 promotes cancer progression via induction of tRNA-derived small RNAs

Zhuojia Chen[2,3], Meijie Qi[4], Bin Shen[4], Guanzheng Luo[3,5], Yingmin Wu[1], Jiexin Li[1], Zhike Lu[3], Zhong Zheng[3], Qing Dai[3] and Hongsheng Wang[1,3,*]

[1]Department of Microbial and Biochemical Pharmacy, Guangdong Provincial Key Laboratory of New Drug Design and Evaluation, School of Pharmaceutical Sciences, Sun Yat-sen University, Guangzhou 510006, China, [2]Sun Yat-sen University Cancer Center; State Key Laboratory of Oncology in South China; Collaborative Innovation Center for Cancer Medicine, Guangzhou 510060, China, [3]Department of Chemistry, The University of Chicago, 929 East 57th Street, Chicago, IL 60637, USA, [4]State Key Laboratory of Reproductive Medicine, Department of Histology and Embryology, Nanjing Medical University, Nanjing 211166, China and [5]School of Life Sciences, Sun Yat-sen University, Guangzhou 510006, China

Received July 24, 2018; Revised November 16, 2018; Editorial Decision November 27, 2018; Accepted December 03, 2018

ABSTRACT

Transfer RNA is heavily modified and plays a central role in protein synthesis and cellular functions. Here we demonstrate that ALKBH3 is a 1-methyladenosine (m^1A) and 3-methylcytidine (m^3C) demethylase of tRNA. ALKBH3 can promote cancer cell proliferation, migration and invasion. *In vivo* study confirms the regulation effects of ALKBH3 on growth of tumor xenograft. The m^1A demethylated tRNA is more sensitive to angiogenin (ANG) cleavage, followed by generating tRNA-derived small RNAs (tDRs) around the anticodon regions. tDRs are conserved among species, which strengthen the ribosome assembly and prevent apoptosis triggered by cytochrome *c* (Cyt *c*). Our discovery opens a potential and novel paradigm of tRNA demethylase, which regulates biological functions via generation of tDRs.

INTRODUCTION

Nowadays, more than 100 forms of modifications have been identified to regulate the biological functions of RNA (1). Transfer tRNA (tRNA), which functions as amino acid carrier during protein synthesis, are heavily modified post-transcriptionally (2). It has been reported that there are 13 modifications, on average, in one human tRNA (3). These modifications can influence the structure, stability and translation accuracy of tRNA (4,5). As reported, a large subset of tRNA modification enzymes are linked to human diseases (6).

Methylation is the most frequently happening post-transcriptional modification of tRNA (7,8). In cytoplasmic tRNA, 1-methyladenosine (m^1A) at position 58 (m^1A58) is the predominant m^1A modification in eukaryotic cells (9). The 3-methylcytidine (m^3C) modification occurs at position 32 in the anticodon loop of cytoplasmic $tRNA^{Thr}$, $tRNA^{Ser}$ and $tRNA^{Arg}$, and also at other positions (20 or 47) of $tRNA^{Leu}$ and $tRNA^{Met\text{-}e}$ (10). Modifications of tRNA are crucial for its stability and biological functions (5). For instance, lack of m^1A58 impairs the hydrogen bonds from A58 to A54 and A60 in initiator $tRNA^{Met}$ of yeast, leading to the degradation of $tRNA^{Met}$ (11). Since tRNA is essential to cellular functions (12), it will be of interest to query which enzyme participates in the dynamic variation of tRNA methylation.

It is well known that tRNA methyltransferases (MTases) such as rossmann-fold MTases (RFM) and SpoU–TrmD MTases (SPOUT) are responsible for tRNA methylation (13). However, demethylase which targets tRNA to remove the methyl group is not well illustrated. FTO and ALKBH5 have been identified as demethylases that catalyze the removal of m^6A modifications in mRNA through an iron-dependent oxidative demethylation mechanism (14). Both FTO and ALKBH5 influence mouse fertility (15), human body weight (16) and cancer progression (17). Recently, m^1A in tRNA was firstly identified that could be demethylated by ALKBH 1 *in vitro* and *in vivo* (18). The dynamic methylation of tRNA affects the cellular level of $tRNA^{iMet}$ and regulates translation initiation (18). Together, it indicates that other AlkB family members might be also involved in the dynamic methylation of tRNA.

Human ALKBH3 belongs to AlkB family that utilizes nonheme iron (II) to catalyze biological oxidation (19). Previous report showed that ALKBH3 prefers to demethylate single-stranded DNA (ssDNA) and RNA (19). Although ALKBH3 has been suggested to be involved in single strand RNA demethylation (20), studies tended to focus its demethylase activity on DNA, such as DNA repair

*To whom correspondence should be addressed. Tel: +86 20 39943024; Email: whongsh@mail.sysu.edu.cn

and genomic stability (21,22). It has been reported that expression of ALKBH3 is elevated in pancreatic (23), lung (24) and urothelial (25) cancer as compared to the normal tissue. Also, ALKBH3 is suggested to benefit the growth and progression of colorectal (26) and lung (24) cancer cells. However, it remained to be elusive whether ALKBH3-modulated DNA/RNA demethylation is involved in its promotion effects on cancer progression.

Here, we found that ALKBH3 acted as tRNA demethylase to remove the methyl group of m^1A and m^3C in tRNA both *in vitro* and *in vivo*. Demethylated tRNA was more sensitive to the cleavage of angiogenin (ANG), which resulted in the generation of tRNA-derived small RNAs (tDRs). The tDRs were involved in ALKBH3-induced cancer progression via promoting ribosome assembly and preventing cell apoptosis.

MATERIALS AND METHODS

Cross-linking immunoprecipitation (CLIP) and sequencing

The CLIP procedures were conducted using HeLa cells according to the previous study (27) with slight modifications. Briefly, four plates of HeLa cells in 15 cm dishes were transfected with pPB/ALKBH3 plasmid for 48 h to reach about 90% cell confluency. After washing twice with ice-cold PBS, cells were irradiated twice with 400 mJ/cm^2 at 254 nm by Stratalinker on ice. Cells were lysed in high salt lysis buffer (300 mM NaCl, 0.2% NP-40, 20 mM Tris–HCl PH 7.6, 0.5 mM DTT, protease inhibitor cocktail (1 tablet/50 ml), and RNase inhibitor (1:200)) at 4°C for 30 min. Supernatant was collected after centrifuged at 17 000 *g* at 4°C for 15 min and further treated with 1 U RNase T1 for 15 min at 24°C. After centrifugation and filtration through 0.22 μM filter, 10% supernatant was collected as input for further sequencing analysis. Anti-Flag M2 beads (Sigma-Aldrich, St. Louis, MO, USA, 80 μl) were washed three times with lysis buffer and incubated with the filtered supernatant at 4°C for 4 h. After removing the flow through by magnetic rack, beads were washed with for three times with 1 ml of high salt buffer (5× PBS supplemented with 0.1% SDS, 1% Nonidet P-40 and 0.5% sodium deoxycholate) and another three times with 1 ml of wash buffer (20 mM Tris–HCl, pH 7.4, 10 mM $MgCl_2$ and 0.2% Tween-20). Beads and input were further incubated with 10 U RNase T1 exactly for 8 min. Then, bead samples were treated with 95 μl commercial PNK buffer and 0.5 U PNK for 15 min at 37°C. After treatments, final concentration of 100 μM ^{32}P-labeled ATP and 1 U PNK were added and incubated at 37°C for another 30 min. The RNA/protein complexes were eluted by NuPAGE 1× loading buffer and fractionated by neutral NuPAGE 4–12% bis–tris gel. The gel contents were transferred to nitrocellulose by wet transfer; the filter was blotted dry and exposed to film. A fraction of the membrane from approximately 40 to 70 kDa was used for purification of the RNA–protein complexes (Supplementary Figure S1E). RNAs were recovered by proteinase K digestion in proteinase K buffer, followed by phenol/chloroform extraction using glycogen as carrier. The RNA fragments were ligated to adapter and established library by NEB small RNA library preparation kit (E7330S). For RNA binding analysis, RNAs were extracted by phenol/chloroform. Next, 50 ng ALKBH3-bound RNAs were separated by TBE-Urea-PAGE. IgG was used as the negative control, while human total tRNA and Bakers yeast tRNA (Sigma 10109495001) were used as a size marker. The TBE-Urea gel was finally visualized by SYBR-Gold.

mRNA, rRNA and mtRNA purification

The mRNA was purified by Ambion Dynabeads® mRNA DIRECT™ Purification Kit twice according to according to the manufacturer's instruction. For rRNA, total RNAs were separated with 1.5% agarose gel, then 18S and 28 S rRNA were recovered from the gel by Zymoclean™ Gel RNA Recovery Kit (Zymo Research, Orange, CA, USA). For mtRNA, the mitochondria were separated by use of the magnetic beads method (Mitochondria Isolation Kit; Miltenyi Biotec, Auburn, CA, USA). Total mtRNA was extracted by Trizol.

In vitro biochemistry assay

The *in vitro* biochemistry assay was conducted according to previous study (28) with slight modifications. Generally, the 50 μl reaction system contained the following components: RNAs (probes), wt or mutant ALKBH3 protein, KCl (100 mM), $MgCl_2$ (2 mM), RNasin (0.2 U μl^{-1}, Invitrogen), L-ascorbic acid (2 mM), α-ketoglutarate (300 μM), $(NH_4)_2Fe(SO_4)_2{\cdot}6H_2O$ (150 μM) and 50 mM of HEPES buffer (pH 7.0). The reactions were incubated at 37°C for 1.5 h, then quenched by addition of 5 mM EDTA and heated at 95°C for 10 min. Samples were then centrifuged at 13 000 *g* for 30 min at room temperature and supernatant was collected for LC–MS/MS analysis. The probes were synthesized in our lab and purified by HPLC. The sequences of the probes were listed as follows:

m^1A in loop RNA: 5′-CCCGGUUCG5UUCCCGG (5 = m^1A, T-loop of $tRNA^{HisGTG}$, loop size 8)
m^1A in linear RNA: 5′-CACGGUUCG5UUCAAAG (5 = m^1A, no second structure)

Cell proliferation, colony formation, invasion and apoptosis

Cell proliferation was tested by CCK-8 kit (Dojindo, Gaithersburg, MD, USA) according to previous studies (17,18). Colony formation was detected by CytoSelect 96-well Cell Transformation Assay (Cell Biolabs, USA). Cell invasion was examined by the CytoSelect™ 24-well extracellular matrix (ECM) array (Cell Biolabs, USA). The apoptosis was detected by FITC annexin V apoptosis detection kit with PI (Biolegend, San Diego, CA, USA).

Polysome profiling

Polysome profiling was performed according to previously stated method (29). The fractions were categorized and used to isolate total RNA by Trizol reagent for RT-PCR, tRNA purification and LC-MS/MS measurement.

tRNA fragment purification and sequencing

Total RNA (100 μg) were denatured at 70°C for 5 min and separated by a 15% TBE–urea gel with 20/100 or 10/60

oligo length standard ladder (Integrated DNA Technologies, Coralville, IA, USA). After visualized by SYBR Gold (Ref. S11494 from Life Technologies), tDRs in gels were cut according to sizes and recovered by small RNA PAGE recovery kit (Zymo Research, Irvine, CA, USA). The tDRs were further treated with Tris for deacylation (30,31) and T4 PNK for RNA end repair according to the previous studies (30,32). The recovered tDRs was used to establish the library by NEB small RNA library preparation kit (E7330S).

Data analysis

The statistical analysis was performed by SPSS 17.0 for Windows. Data were analyzed by two-tailed unpaired Student's *t*-test between two groups. $^{*}P < 0.05$, $^{**}P < 0.01$. All other methods are described in detail in the supplementary data.

RESULTS

ALKBH3 localizes in cytoplasm and links to tRNA *in vivo*

The specificity of a commercial available anti-ALKBH3 antibody (Millipore, 09882) was confirmed by western blot analysis, which showed that the antibody can specifically detect a single protein band with the expected size of ∼35 kDa, corresponding to the endogenous and exogenous (over expression, o/e) ALKBH3 (Supplementary Figure S1A). Next, the cellular localization of ALKBH3 in various cell lines was analyzed by immunofluorescence assay. In tested cells including *293T*, *HeLa*, *HepG2*, *DU145* and *PC3* cells, ALKBH3 is dominant in cytoplasm (Figure 1A). Localization of ALKBH3 in cytoplasm was further confirmed by western blot analysis (Supplementary Figure S1B). Consistent results were observed in cells transiently overexpressing ALKBH3, which were stained by Flag antibody (Supplementary Figure S1C). Western blot analysis showed that ALKBH3 was detected in various human cells (Supplementary Figure S1D). Collectively, our data suggested that ALKBH3 was widely expressed in human cancer cells and predominantly located in the cytoplasm.

Considering that RNA is one of substrates of ALKBH3 (19), we then utilized crosslinking and immunoprecipitation sequencing (CLIP-seq) to classify the potential RNAs bound by ALKBH3 (Supplementary Figure S1E). The CLIP-seq data showed that tRNA was the most significantly enriched RNA in ALKBH3-based CLIP products compared to the input (Figure 1B, Supplementary Figure S1F). All ALKBH3-bound RNAs were separated by TBE-urea denaturing gel and visualized by SYBR gold staining. Results consistently showed that tRNA was the major RNA type bound by ALKBH3 in HeLa cells (Figure 1C). CLIP-Seq results revealed that the composition of tRNA bound by ALKBH3 was different from that of the total RNA input (Figure 1D, Supplementary Table S1). The tRNA which showed over 30 in enrichment folds (CLIP versusinput) and over 0.5% in relative abundance in CLIP group included $tRNA^{GlyGCC}$, $tRNA^{GlnCTG}$, $tRNA^{HisGCG}$, $tRNA^{GlyCCC}$, $tRNA^{SerGCT}$ and $tRNA^{LysCTT}$ (Figure 1D, Supplementary Figure S1G). Furthermore, protein sequence alignment between ALKBH3 and the tRNA-binding motifs of ALKBH1, a known tRNA demethylase (18), was performed. Results indicated that ALBKH3 contained a similar tRNA-binding domain as ALKBH1, which may function as tRNA recognition (Supplementary Figure S1H). Collectively, our data suggested that ALKBH3 can recognize and bind to tRNA *in vivo*.

ALKBH3 catalyzes demethylation of m^1A and m^3C in tRNA

Since CLIP-seq suggested that ALKBH3 was associated to tRNA *in vivo*, we hypothesized that the known tRNA methylations such as m^7G, m^1G, m^1A, m^5C and m^3C, might be the target of ALKBH3. *In vitro* biochemical assay showed that ALKBH3 significantly decreased the levels of m^1A and m^3C, but not others, in tRNAs from both HeLa (Figure 2A) and *293T* (Supplementary Figure S2A) cells. Similar observations were obtained using the commercial tRNA from bakers yeast (Sigma, Cat. 10109495001) (Supplementary Figure S2B). ALKBH3 had no effect on the modifications including f^6A, m^6Am, Am, Cm, Gm, Um or Ca^5C in tRNAs from HeLa cells (data not shown). Besides, enzymatic kinetic studies using purified tRNA and synthesized RNA probes showed that ALKBH3 rapidly (2 min) demethylated m^1A and m^3C of tRNA *in vitro*, effect of which is comparable to the m^1A demethylation activity of ALKBH1 (18). Moreover, m^1A demethylation activity of ALKBH3 tended to be higher on tRNA and loop RNA probes than that of linear RNA probe (Figure 2B).

To evaluate the demethylation effects of ALKBH3 *in vivo*, HeLa cells were transfected with pcDNA/AKLBH3 or si-ALKBH3 1∼3 (Supplementary Figure S2C). Overexpression of ALKBH3 led to a significant decrease in m^1A (16%) and m^3C (26%) of total tRNA after 24 h transfection (Figure 2C and D). Meanwhile, knockdown of ALKBH3 by si-ALKBH3-1∼3 remarkably increased m^1A (17∼24%) and m^3C (20∼45%) of total tRNA (Figure 2C and D). Similar observations were obtained in *293T* cells (Supplementary Figure S2D). Furthermore, 16% and 21% reductions of m^1A and m^3C levels in total tRNAs, respectively, were detected in HeLa cells stably overexpressing ALKBH3 (Supplementary Figure S2E). Consistently, increase of m^1A (15%) and m^3C (12%) levels in tRNAs from *Alkbh3*$^{-/-}$ cells were observed when compared to that from wild-type HeLa cells (Supplementary Figure S2E).

We further tested the functions of ALKBH3 in wild type (WT) and *Alkbh3*$^{-/-}$mice. The high to low expression levels of ALKBH3 in organs of wide type mice was lung, testis, epididymis, liver, kidney and heart (Supplementary Figure S2F). The levels of m^1A (Figure 2E) and m^3C (Figure 2F) in tRNAs isolated from lung, testis, epididymis of *Alkbh3*$^{-/-}$mice were significantly ($P < 0.05$) enhanced. However, there was no statistical difference for m^1A or m^3C in liver, kidney or heart between WT or *Alkbh3*$^{-/-}$mice (Supplementary Figure S2G). We next examined the potential effects of ALKBH3 on mRNA, rRNA or mtRNA (mitochondria RNA). Our data showed that ALKBH3 was independent to the m^1A of mRNA (Supplementary Figure S2H), rRNA (Supplementary Figure S2I) or mtRNA (data now shown) in tested cells.

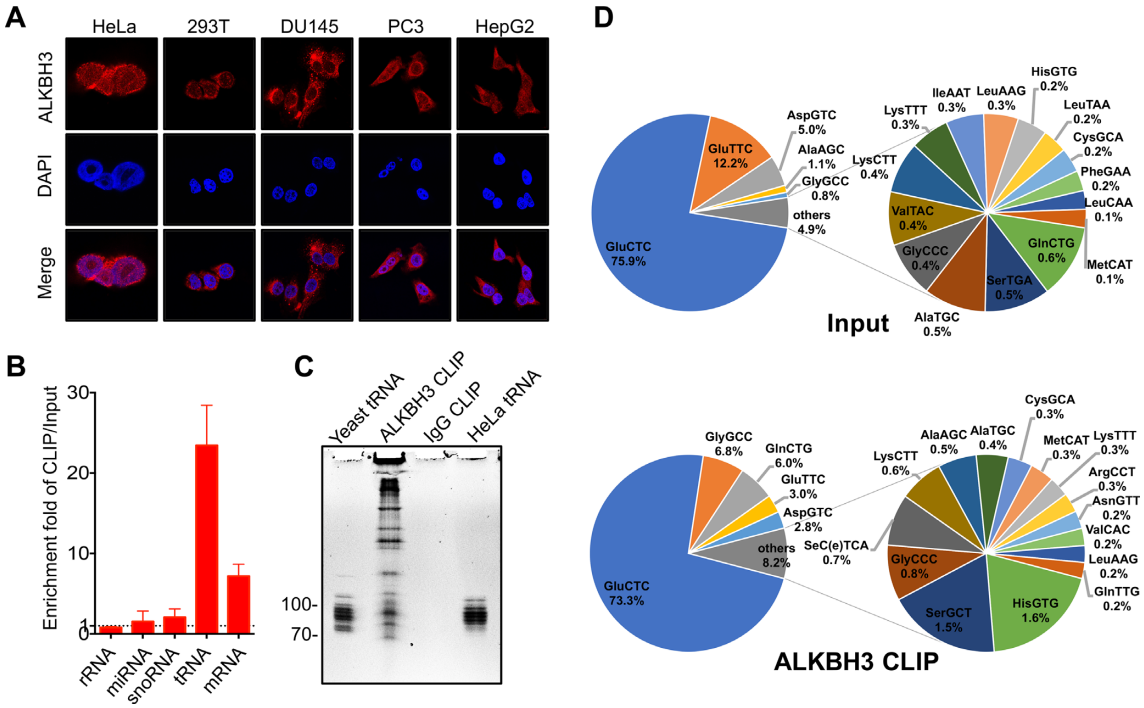

Figure 1. *ALKBH3 localizes in cytoplasm and links to tRNA in vivo.* (**A**) Immunofluorescence staining of endogenous ALKBH3 (*red*) was performed using anti-ALKBH3 antibody. Nuclei were counter-stained by DAPI (*blue*); (**B**) the relative enrichment folds of identified RNA types in ALKBH3-CLIP samples compared to that of the total input samples (CLIP/input of rRNA was used for normalization of other RNAs); (**C**) ALKBH3-bound RNAs in HeLa cells. Bakers yeast tRNA (Sigma 10109495001) and purified human tRNA were used as size marker. IgG was used as the negative control; (**D**) pie chart showing the identified top 20 specific tRNAs in ALKBH3-CLIP samples and input samples (two replicates for each group). See also Supplementary Figure S1.

Characterization and catalytic properties of ALKBH3 on specific tRNA

ALKBH3 acting as demethylase on tRNA was further characterized. *In vitro* pulldown assays confirmed that ALKBH3 showed favoritism to m^1A and m^3C than A or C of ssRNA probe (Supplementary Figure S3A). To better understand the demethylation activity, two ALKBH3 mutants were constructed, which were defective in its DNA/RNA binding groove residue Arg122 or central position at the active site Leu177, respectively, via Ala substitutions (Supplementary Figure S3B). Results showed that both R122A and L177A mutants lost their demethylation activity on m^1A of tRNA *in vitro* (Figure 3A) and *in vivo* (Supplementary Figure S3C). This was consistent with previous data that Arg122 and Leu177 were essential to the ALKBH3 activity (33).

The subcellular targets of ALKBH3 were further investigated. Our data showed that in *Alkbh3*$^{-/-}$ HeLa cells, m^1A level of tRNA in cytoplasm, but not in nucleus, was remarkably higher than that of wild type cells (Figure 3B). Similar results were observed in HeLa cells stably overexpressing ALKBH3 (Supplementary Figure S3D). This might be due to that ALKBH3 predominantly located in the cytoplasm. Next, we divided tRNA into two fractions, translation initiation fraction (containing 40S ribosomes, 60S ribosomes, 80S monosomes, <80S) and translation activing fraction (containing polysomes, > 80S), from HeLa cells by use of ribosome profiling (Figure 4F). The tRNA content in <80S fraction was much greater than that of >80S fraction (Supplementary Figure S3E). LC–MS/MS (Figure 3C) and northern blot analysis (Supplementary Figure S3F) showed that m^1A level of tRNA in <80S fraction, but not > 80S fraction, was significantly increased in *Alkbh3*$^{-/-}$ HeLa cells. In addition, northern blot analysis indicated that m^1A modification mainly existed in tRNA (Supplementary Figure S3F).

We further validated the demethylation activity of ALKBH3 on selected tRNA. Gel-images showed that individual tRNAs were successfully purified and identical in wild type and *Alkbh3*$^{-/-}$ HeLa cells (Supplementary Figure S3G). LC/MS/MS showed that deletion of ALKBH3 significantly increased the m^1A levels of most target tRNAs such as $tRNA^{GluCTC}$, $tRNA^{SeCTCA}$, $tRNA^{GlyGCC}$, $tRNA^{HisGTG}$, $tRNA^{SerGCT}$, $tRNA^{GlnCTG}$, $tRNA^{ValCAC}$, $tRNA^{ArgCCT}$, $tRNA^{LeuCAA}$, $tRNA^{GlyCCC}$, $tRNA^{AlaCGC}$ and $tRNA^{eMetCAT}$. However, m^1A levels of some targets, such as $tRNA^{LysCTT}$ and $tRNA^{AsnGTT}$, were not affected by ALKBH3. $tRNA^{iMet}$ or $tRNA^{PheGAA}$ was not the target of ALKBH3. As expected, no significant effect of ALKBH3 on their m^1A levels was detected (Figure 3D). *In vitro* biochemical assay showed ALKBH3 reduced the m^1A levels of its targets such as $tRNA^{GluCTC}$, $tRNA^{GlyGCC}$, $tRNA^{HisGTG}$, $tRNA^{GlnCTG}$, $tRNA^{ValCAC}$, $tRNA^{ArgCCT}$, $tRNA^{LeuCAA}$ and $tRNA^{AlaCGC}$ (Supplementary Figure S3H).

Besides, m^3C levels of target tRNA were significantly up-regulated in *Alkbh3*$^{-/-}$ HeLa cells, including $tRNA^{SerGCT}$, $tRNA^{ArgCCT}$, $tRNA^{LeuCAA}$ and $tRNA^{eMetCAT}$ (Figure 3E). We conducted primer extension analysis for

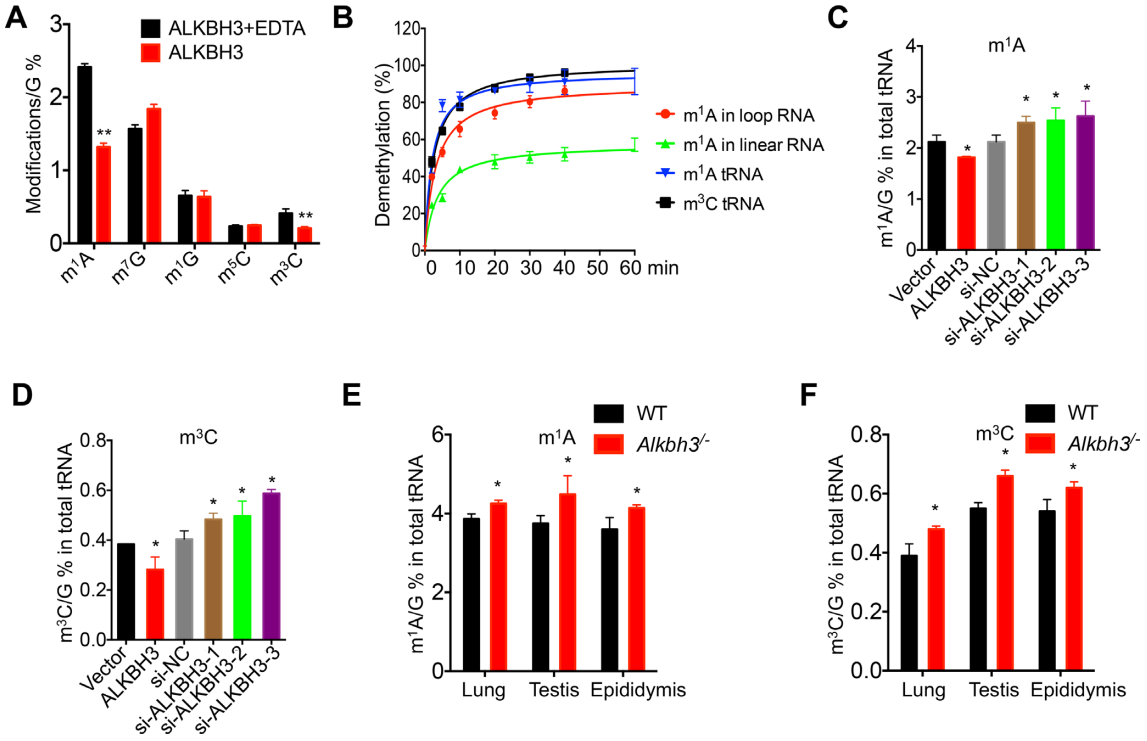

Figure 2. *ALKBH3 catalyzes demethylation of m^1A and m^3C in tRNA*. (**A**) Total tRNAs were purified from HeLa cells and incubated with ALKBH3 protein or ALKBH3 protein + EDTA for 1 h (EDTA chelates cofactor iron and inactivates ALKBH3); (**B**) Michaelis–Menten plot of the steady-state kinetics of ALKBH3-catalyzed demethylation in stem-loop structured RNA probes that mimic the TΨC loops of $tRNA^{His(GUG)}$, linear RNA probe and tRNA purified from HeLa cells at pH 7.5 at 37°C; (C, D) HeLa cells transfected with pcDNA (Vector) or pcDNA/ALKBH3 for 24 h, or siRNA negative control (si-NC) and si-ALKBH3–1∼3 for 48 h. Total tRNAs were then purified and digested for HPLC-MS/MS measurements of m^1A (**C**) and m^3C (**D**); (E, F) The relative levels of m^1A (**E**) and m^3C (**F**) of total tRNAs from lung, testis and epididymis of wide type or *Alkbh3*$^{-/-}$mice. Data were presented as means ± SD from three independent experiments. *$P < 0.05$ compared with control; **$P < 0.01$ compared with control. See also Supplementary Figure S2.

tRNA-GlyGCC, tRNA-ArgCCT and tRNA-SerGCT according the published protocol (34). In ALKBH3 stable overexpressing HeLa cells, a decrease in m^1A and/or m^3C allows for readthrough and an extended product up to a subsequent RT-blocking modification, such as 1-methylguanosine (m^1G) or dimethylguanosine ($m^2{}_2G26$).

As shown in Supplementary Figure S3I, we identified a reverse transcription (RT) block at the expected position of each tested tRNA in control cells. In contrast, the RT block at position at m^1A58 of GlyGCC, m^3C32 of ArgCCT, m^3C32/m^3C47 of SerGCT (10) was completely absent from ALKBH3 stable overexpressing HeLa cells. These results showed that m^1A58, m^3C32 and m^3C47 in tRNA can be regulated by ALKBH3.

The expression levels of ALKBH3-regulated tRNA were verified by northern blot analysis, showing that deletion of ALKBH3 had no obvious effect on the expression of most target tRNAs expect $tRNA^{GlyGCC}$, which showed a slight up-regulation. Notably, deletion of ALKBH3 was independent to the expression of $tRNA^{iMet}$, which is crucial to translation initiation (Supplementary Figure S3J).

The promotion effects of ALKBH3 on cancer progression

ALKBH3 contributed to survival and growth of cancer cells via yet-to-be illustrated mechanisms (21,25,35). We found that knockdown of ALKBH3 significantly inhibited the proliferation of *HeLa*, *PC3*, *DU145* and *HepG2* cells (Supplementary Figure S4A). Moreover, the *Alkbh3*$^{-/-}$ HeLa cells showed a significant reduction in cell proliferation (Figure 4A), colony formation (Figure 4B) and invasion capability (Figure 4C) when compared with the wild type cells. Consistently, HeLa cells stably overexpressing ALKBH3 showed remarkable promotion effects on cell proliferation, colony formation and invasion (Supplementary Figure S4B∼D). The *Alkbh3*$^{-/-}$ HeLa cells were more sensitive to chemotherapy drug doxorubicin (Dox) than that of wild type cells (Supplementary Figure S4E). The IC_{50} values of Dox in wild type and *Alkbh3*$^{-/-}$ HeLa cells were 2.51 and 1.22 μM, respectively. Similarly, *Alkbh3*$^{-/-}$ cells were more susceptible to cell stress induced by sodium arsenite (Supplementary Figure S4F). Taken together, ALKBH3 positively regulated proliferation, colony formation, and invasion of cancer cells.

We further investigated the potential *in vivo* effects of ALKBH3 on cancer progression. Both wild type and *Alkbh3*$^{-/-}$ HeLa cells were injected subcutaneously into nude female mice. At the end of the experiments, tumor growth and volumes were significantly lower in mice injected with *Alkbh3*$^{-/-}$ HeLa cells compared to those injected with wild type cells (Figure 4D). IHC results also suggested that ALKBH3 depletion led to a lower level of Ki67 in xenograft tumor tissues (Figure 4E). Significant in-

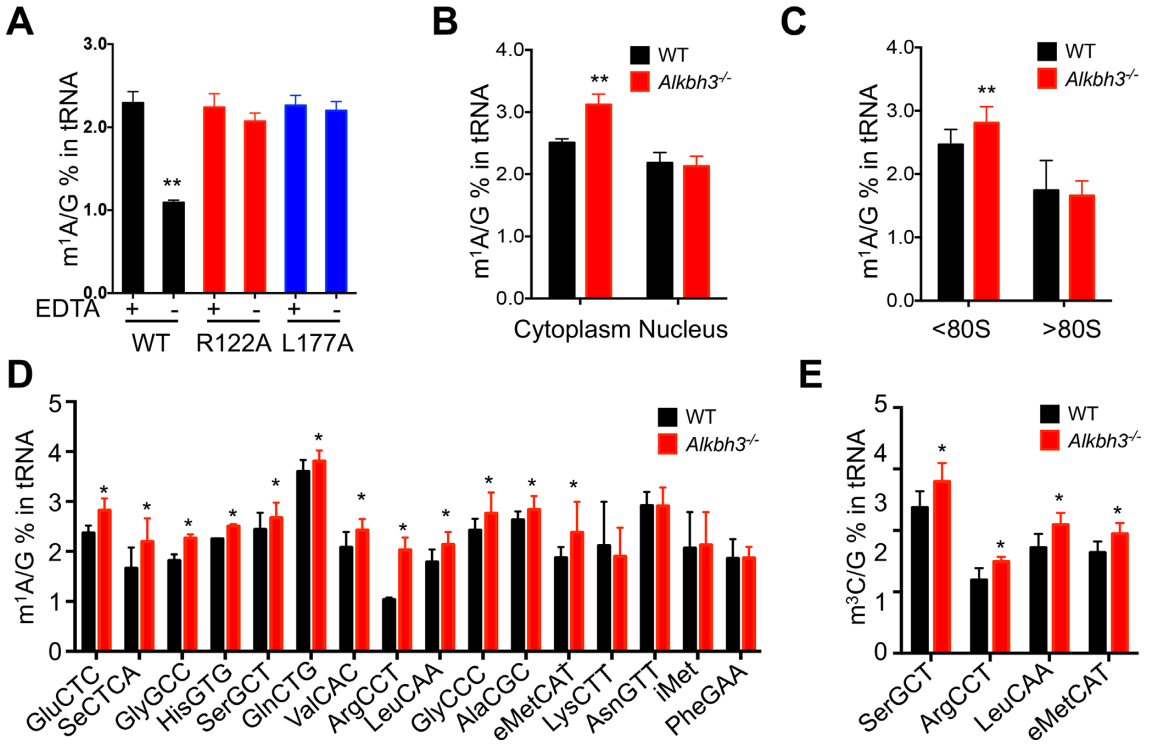

Figure 3. *Characterization and catalytic properties of ALKBH3 on specific tRNA.* (**A**) *In vitro* biochemical assays of ALKBH3 wild type (WT), mutant R122A or mutant L177A in total tRNA of HeLa cells at 37°C for 1 h (EDTA chelates cofactor iron and inactivates ALKBH3); (**B**) the m^1A levels of tRNA in cytoplasm and nucleus isolated from wild type (WT) and *Alkbh3*$^{-/-}$ HeLa cells, respectively; (**C**) the m^1A levels of tRNA isolated from the translation initiation non-polysome fractions (<80S, containing 40S ribosome, 60S ribosome and 80S monosome) and translation activing fraction (>80S, containing polysomes) from wild type (WT) and *Alkbh3*$^{-/-}$ HeLa cells, respectively; (**D**) levels of m^1A in specific tRNA from wild type (WT) and *Alkbh3*$^{-/-}$ HeLa cells, pulled down by corresponding cDNA probes; (**E**) levels of m^3C in specific tRNA from wild type (WT) and *Alkbh3*$^{-/-}$ HeLa cells, pulled down by corresponding cDNA probes; Data were presented as means ± SD from three independent experiments. *$P < 0.05$ compared with control. **$P < 0.01$ compared with control. See also Supplementary Figure S3.

creased expression of ALKBH3 in cervical cancer versus normal tissues has been observed in Biewenga (Supplementary Figure S4G) and Pyeon (Supplementary Figure S4H) data from Oncomine database.

We evaluated effects of ALKBH3 on protein synthesis and translation. Confocal showed a lower synthesis rate of nascent proteins in *Alkbh3*$^{-/-}$ cells as compared with that in wild type cells (Figure 4F). Consistently, stable overexpression of ALKBH3 enhanced the protein synthesis rate (Supplementary Figure S4I). Polysome profiling showed that deletion of ALKBH3 decreased the 80S monosome and polysome content, suggesting that protein synthesis process was delayed (Figure 4G). Since $tRNA^{iMet}$ was not the target of ALKBH3 according to the results of CLIP-seq and mass spectrum, we investigated the roles of ALKBH3 in tRNA-mediated elongation during protein translation. It is achieved by a reporter that six repeated specific codon sequences (6× CAC for $tRNA^{HisGTG}$, 6× GGC for $tRNA^{GlyGCC}$ and 6× GAC for $tRNA^{GlnCTG}$) were added in the front of 5′ end of firefly luciferase (F-luc) (18), so that the elongation rate was detected as the fluorescence signal of F-luc (Figure 4H). However, there was no significant difference in the luciferase translation of 6× CAC(His), 6× GGC(Gly) or 6× CAG(Gln) between wild type and *Alkbh3*$^{-/-}$ cells (Figure 4I). Considering that upregulation of $tRNA^{GlyGCC}$ was observed in *Alkbh3*$^{-/-}$ HeLa cells, we blocked its function in cells by transfection a reverse complimentary RNA which can target the anti-codon region of $tRNA^{GlyGCC}$ according to the previous study (36). However, blocking of $tRNA^{GlyGCC}$ had no effect on growth inhibition of *Alkbh3*$^{-/-}$ cells (Supplementary Figure S4J). Data above indicated that ALKBH3-triggered cancer progression might be independent to the translational functions of tRNA.

ALKBH3 catalyzes generation of tDRs via an ANG-dependent manner

Demethylation of tRNA can suppress tRNA stability and trigger the generation of tDRs (37,38). tDRs are associated to cancer progression via increasing cell proliferation in breast and prostate cancers (32). Thus, we hypothesized that ALKBH3 may regulate the generation of tDRs in cancer cells. Small RNAs (smRNA) ranging from 15 to 50 bp from wild type and *Alkbh3*$^{-/-}$ mice epididymis was recovered by TBE–urea gel (Supplementary Figure S5A) and subjected to Illumina ultra-high–throughput sequencing (Supplementary Table S2). Data showed that tDRs was the predominant RNA type in smRNA pool from both wild type and *Alkbh3*$^{-/-}$ mice epididymis, however, percentage of tDRs decreased from 44.4% in wild type to 37.2% in *Alkbh3*$^{-/-}$ mice (Figure 5A). Similar composition profiles of tDR were observed in both wild type and

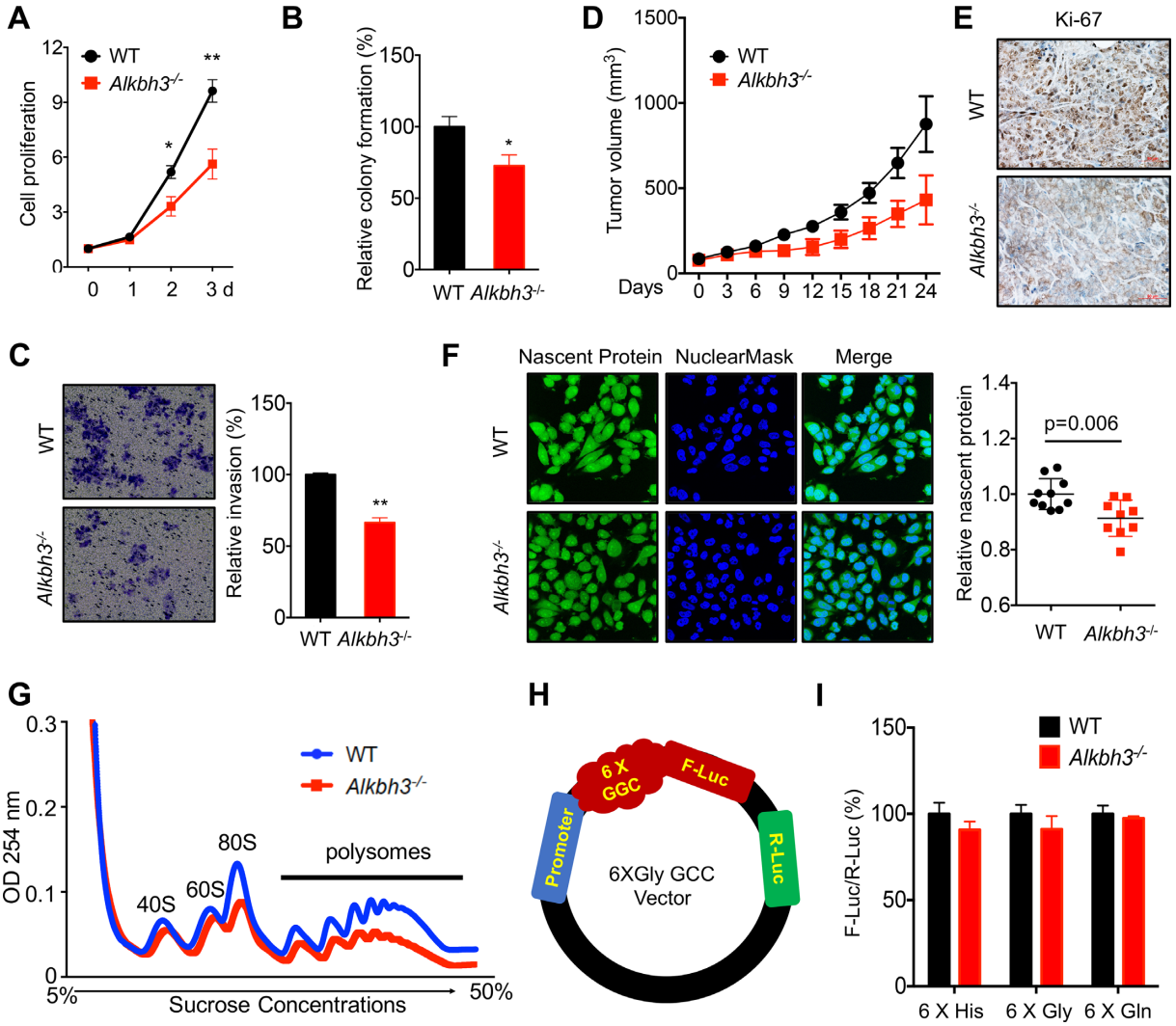

Figure 4. *The promotion effects of ALKBH3 on cancer progression.* (**A**) The relative cell proliferation of wild type (WT) vs *Alkbh3*$^{-/-}$ HeLa cells were measured by CCK-8 kit; (**B**) cells were seeded in soft agar in a 96-well plate, grown for a week and soft agar colony formation was measured; (**C**) *in vitro* invasion assay of wild type (WT) versus *Alkbh3*$^{-/-}$ HeLa cells for 24 h; (**D**) tumor growth curves of wild type (WT) versus *Alkbh3*$^{-/-}$ HeLa cells in xenograft models at the indicated time interval; (**E**) IHC (Ki67)-stained paraffin-embedded sections obtained from xenografts. Red bar = 50 μm. (**F**) The wild type (WT) or *Alkbh3*$^{-/-}$ HeLa cells were replaced with methionine-free medium supplemented with methionine analog HPG and incubated for 1 h. HPG incorporation was measured by confocal microscope, quantitatively analyzed the intensity of fluorescence, and normalized to nucleus (NuclearMask); (**G**) The polysome profiling of wild type (WT) or *Alkbh3*$^{-/-}$ HeLa cells were analyzed; (H) Representative scheme of the reporter assay: the RNA reporter vector encodes firefly luciferase (F-luc) as the primary reporter and Renilla luciferase (R-luc) on the same plasmid as the internal transfection control. 6× CAC (His), 6× GGC (Gly) or 6× CAG (Gln)-coding sequences (recognized by $tRNA^{HisGTG}$, $tRNA^{GlyGCC}$ and $tRNA^{GlnCTG}$, respectively) were inserted after the PLK promoter region. (**I**) Positive and control reporter were transfected into wild type (WT) or *Alkbh3*$^{-/-}$ HeLa cells for 24 h. The control reporter without any insertion was used to normalize the translation differences between the two cells lines. Data were presented as means ± SD from three independent experiments. The cell proliferation was replicated six times for each group. *$P < 0.05$, **$P < 0.01$ compared with control. See also Supplementary Figure S4

Alkbh3$^{-/-}$ mice epididymis (Figure 5B). Since the RPM (Reads per million total reads) of 5′-tDR in epididymis of wild type mice was 24-fold greater than that of 3′-tDR, we only focused on the potential roles of 5′-tDRs in the next study. Among them, 5′tDR-GlyGCC was the most abundant tDRs in *Alkbh3*$^{-/-}$ mice epididymis, followed by 5′tDR-GlyCCC, 5′tDR-ValCAC, 5′tDR-HisGTG and 5′tDR-GlnCTG (Supplementary Figure S5B). Norther blot analysis (Figure 5C) and TaqMan qRT-PCR (Supplementary Figure S5C) showed that the expression of 5′tDR-GlyGCC was decreased in epididymis, testis and lung of *Alkbh3*$^{-/-}$ mice than that of WT mice. As shown in Figure 5D, 5′tDR-GlyGCC was derived from np 1–30–32 of mature $tRNA^{GlyGCC}$. Similarly, other ALKBH3-regulated tDRs, including 5′tDR-GlyCCC, 5′tDR-ValCAC and 5′tDR-HisGTG, were also derived from np 30–33 of their corresponding mature tRNAs (Supplementary Figure S5D). Since overexpression of ALKBH3 had no significant effect on the expression of tDRs from m^3C-containing tRNAs including $tRNA^{SerGCT}$, $tRNA^{ArgCCT}$, $tRNA^{LeuCAA}$ and $tRNA^{eMetCAT}$, m^1A demethylation is the most likely reason for ALKBH3-induced generation of tDRs.

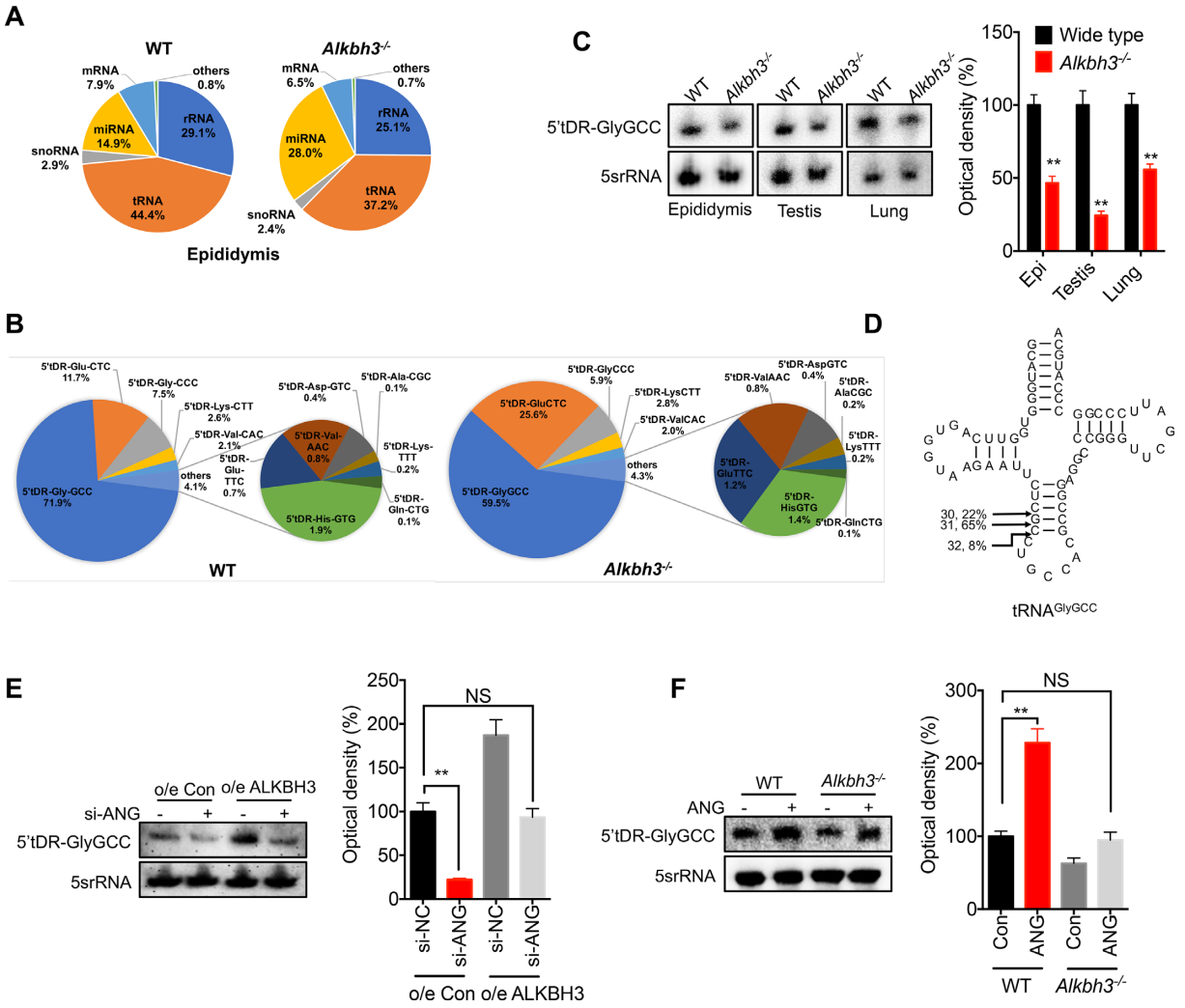

Figure 5. *ALKBH3 catalyzes generation of tDRs via an ANG-dependent manner.* (**A**) All smRNAs from WT or *Alkbh3*$^{-/-}$mice epididymis were purified and subjected to Illumina ultra-high–throughput sequencing (n = 2). The smRNAs were mapped to miRNAs, tRNAs, rRNAs or mRNA transcripts and normalized to the total reads; (**B**) pie chart showing the identified top 12 individual tDRs in WT or *Alkbh3*$^{-/-}$mice epididymis; (**C**) the 5′tDR-GlyGCC of lung, testis and epididymis from WT or *Alkbh3*$^{-/-}$mice was detected by northern blot analysis using biotin labeled probe (left) and quantitatively analyzed (right); (**D**) major cleavage sites and their corresponding percentages of cleaved tRNA^{GlyGCC} in wild type mice epididymis; (**E**) after transfected with si-ANG or negative control (si-NC) for 24 h, the 5′tDR-GlyGCC from stably overexpressing ALKBH3 and control HeLa cells were detected by northern blot analysis using biotin labeled probe (left) and quantitatively analyzed (right); (**F**) the purified tRNA (500 ng) of WT or *Alkbh3*$^{-/-}$mice epididymis was further treated with 100 ng ANG for 2 h. The production of 5′tDR-GlyGCC was detected by northern blot analysis using biotin labeled probe (left) and quantitatively analyzed (right). Data were presented as means ± SD from three independent experiments. $^{**}P < 0.01$ compared with control. NS, no significant. See also Supplementary Figure S5.

We also sequenced the tDRs in HeLa cells stably overexpressing ALKBH3 and control cells (Supplementary Table S3). Consistently, overexpression of ALKBH3 enhanced the generation of tDRs in HeLa cells. The order of abundance from high to low was: 5′tDR-GlyGCC, 5′tDR-HisGTG, 5′tDR-GlyCCC and 5′tDR-GlnCTG (Supplementary Figure S5E). Notably, the top 10 abundant tDRs in HeLa cells (Supplementary Figure S5F) were consistent to those in mouse epididymis. Northern blot analysis (Figure 5E) and TaqMan qRT-PCR (Supplementary Figure S5G) confirmed overexpression of ALKBH3 can induce the up-regulation of 5′tDR-GlyGCC in HeLa cells. Furthermore, overexpression of ALKBH3 increased the expression of 5′tDR-GlyCCC, 5′tDR-GlnCTG and 5′tDR-HisGCT according to TaqMan qRT-PCR assay (Supplementary Figure S5H).

Angiogenin (ANG) has been reported to mediate tRNA cleavage via a highly regulated process (39), while methylation of tRNA can protect tRNA against this cleavage (40). We then knocked down the expression of ANG via specific siRNAs (Supplementary Figure S5I) to investigate whether ANG is involved in ALKBH3-induced tDRs generation. Northern blot analysis (Figure 5E) and TaqMan qRT-PCR (Supplementary Figure S5G) showed si-ANG attenuated the ALKBH3-induced up-regulation of 5′tDR-GlyGCC in HeLa cells. Meanwhile, ANG treatment synergistically increased the expression of 5′tDR-GlyGCC in HeLa cells stably overexpressing ALKBH3 (Supplementary

Figure S5J). Further, *in vitro* biochemical assay revealed that $tRNA^{GlyGCC}$ isolated from *Alkbh3*$^{-/-}$ mice epididymis was more resistant to ANG cleavage than that from wild type mice (Figure 5F and Supplementary Figure S5K). Together, our results indicated that ALKBH3-induced m^1A demethylation was involved in the generation of tDRs via an ANG-dependent manner.

tDRs are involved in ALKBH3-induced cancer progression

tDRs are functionally diverse and associated to the regulation of gene expression, RNA processing and cancer cell proliferation (32,41,42). The synthesized 5′tDR-GlyGCC, which is the most abundant tDR induced by ALKBH3, promoted the proliferation of wild type HeLa cells and attenuated the suppression effects of *Alkbh3*$^{-/-}$ cells on proliferation (Figure 6A). Consistently, knockdown of 5′tDR-GlyGCC by its specific siRNAs according to the previous study (32) (Supplementary Figure S6A) suppressed the proliferation of *HeLa*, *PC3* and *DU145* cells (Supplementary Figure S6B). Besides, synthesized 5′tDR-GlyGCC promoted protein synthesis in HeLa cells (Figure 6B and Supplementary Figure S6C). These data suggested that 5′tDR-GlyGCC was involved in ALKBH3-induced cancer progression.

To investigate the potential mechanisms of how tDRs regulate cancer progression, we evaluated the subcellular distribution of tDRs in cells. TaqMan qRT-PCR results showed that the expression of 5′tDR-GlyGCC in cytoplasm was much higher than those in nucleus (Supplementary Figure S6D). Polysome profiling combining with TaqMan qRT-PCR showed that 5′tDR-GlyGCC tended to be distributed in <80S fraction rather than > 80S fraction (Supplementary Figure S6E). Similarly, the expression of 5′tDR-GlyGCC in the <80S fraction, rather than >80S fraction, in HeLa cells stably overexpressing ALKBH3 was significantly greater than that in control cells (Supplementary Figure S6F). These results were in line with the finding that ALKBH3 mainly demethylated tRNAs in <80S fraction (Figure 4C). Moreover, the expression of 5′tDR-GlyGCC in 40S portion was significantly greater than that in 60S or 80S portion of ribosome (Figure 6C).

Proteins interacting with tDRs were isolated using biotin-labeled 5′tDR-GlyGCC, 5′tDR-GlnCTG and analyzed by protein mass spectrometry. The main reasons for chosen of 5′tDR-GlnCTG were as following: (i) it showed promotion effect on cell proliferation (Supplementary Figure S6B&G); (ii) it was generated at the other side of anticodon regions within 40∼50 nt length (41 nt) (Supplementary Figure S5D). By using a non-functional RNA as control, we confirmed that both biotin-labeled 5′tDR-GlyGCC and 5′tDR-GlnCTG can trigger cell proliferation (Supplementary Figure S6H). Next, 18 extra proteins were precipitated by both 5′tDR-GlyGCC and 5′tDR-GlnCTG (Figure 6D, Supplementary Figure S6I), compared to the control. Among them, 12 proteins were related to RNA binding, including 40S ribosomal protein S21 (RPS21), nucleophosmin (NPM1), 60S ribosomal protein L26 (RPL26), H/ACA ribonucleoprotein complex subunit 4 (DKC1) and elongation factor 1-alpha 1 (EEF1A1). According to the STRING database (Supplementary Figure S6J), RPS21 and RPL26 are two compositions of eukaryotic ribosome, while Box H/ACA small nucleolar ribonucleoprotein (snoRNP) is involved in rRNA folding via site-specific pseudouridylation. RPS21 immunopreciptitation (IP) and TaqMan qRT-PCR confirmed the direct interaction between tDRs and RPS21 *in vivo* (Figure 6E), which showed significant enrichments of RPS21 in IP-groups of both 5′tDR-GlyGCC and 5′tDR-GlnCTG. It indicated that tDRs may interact with RNA binding proteins or ribosome to regulate translation process.

We employed IRES reporter assay to investigate the mechanisms of how tDRs participate in protein translation (29,43). Three commonly used IRES reporters (HCV IRES, EMCV IRES and CrPV IRES) were introduced individually in the front of F-Luciferase to report the protein translation. HCV IRES bypasses the eIF4 complex and eIF4G-induced loop formation by directly recruiting 40S and eIF3; EMCV IRES directly binds to eIF4G subunit of the eIF4 complex; while CrPV IRES recruits the ribosome completely independent of initiation factors (eIFs) (29,43). Our found that translation of HCV IRES reporter showed a 57% drop in *Alkbh3*$^{-/-}$ cells compared to that in wild type cells (Figure 6F), while the EMCV or CrPV IRES reporter was not affected. Further, both 5′tDR-GlyGCC and 5′tDR-GlnCTG increased HCV IRES-dependent translation (Figure 6G). Together with the results that assembly of 80S monosome was suppressed in *Alkbh3*$^{-/-}$ cells (Figure 4G), our data indicated that ALKBH3-induced tDRs can promote the translation, which likely relies on the direct recruitment of 40S ribosome.

Interestingly, mass spectrometry indicated that both 5′tDR-GlyGCC and 5′tDR-GlnCTG interacted with cytochrome *c* (Cyt *c*), which protects cells from apoptosis (44). Interactions between tDRs and Cyt *c* were further verified by immunopreciptitation and TaqMan qRT-PCR assay (Supplementary Figure S6K). Moreover, flow cytometry showed that cells transfected with 5′tDR-GlyGCC were more resistant to stress-induced apoptosis (Figure 6H). Western blot analysis also confirmed that stress-induced caspase-3 cleavage was attenuated by transfection of 5′tDR-GlyGCC (Figure 6I). Collectively, these data indicated that the interaction between tDRs and Cyt *c*, which prevents cell apoptosis, was involved in ALKBH3-induced cancer progression.

DISCUSSION

We presented herein a systematic study that ALKBH3 acted as a tRNA demethylase to catalyze the demethylation of m^1A and m^3C in tRNA, followed by triggering the generation of tDRs. ALKBH3 was widely expressed by cancer cells and mainly located in cytoplasm with strong binding capability to tRNA. It potently and selectively processed demethylation of m^1A and m^3C of tRNA both *in vitro* and *in vivo*. We found that ALKBH3 triggered cancer progression, including cell proliferation, migration, protein synthesize and drug sensitivity. Results showed that m^1A demethylated tRNAs are more sensitive to ANG treatment and tended to generate tDRs around their anticodon regions. These tDRs can strengthen the ribosome assembly and prevent apoptosis of cancer cells (Figure 7). Our discov-

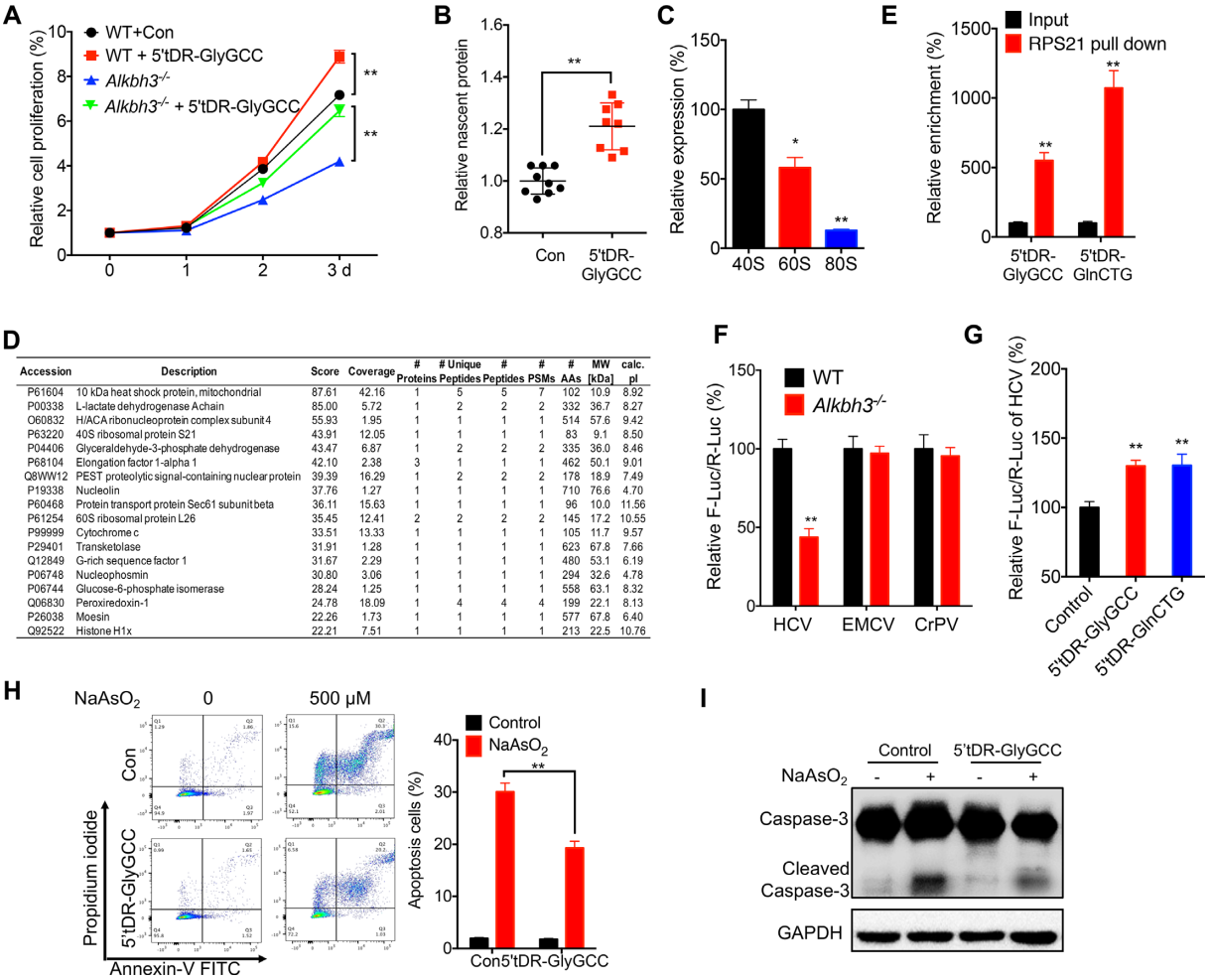

Figure 6. *tDRs are involved in ALKBH3-induced cancer progression.* (**A**) Wild type (wt) or *Alkbh3*$^{-/-}$ HeLa cells were transfected with scrambled control RNA or synthesized 5′tDR-GlyGCC (31 nt) with the final concentration of 50 nM for the indicated times, and the cell proliferation was detected by CCK-8 kit; (**B**) HeLa cells transfected with scrambled control RNA or synthesized 5′tDR-GlyGCC (31 nt) for 24 h were replaced with methionine-free medium supplemented with methionine analog HPG and incubated for 1 h. HPG incorporation was measured by confocal microscope, quantitatively analyzed the intensity of fluorescence, and normalized to nucleus (NuclearMask); (**C**) the ribosome fractions of HeLa cells were grouped to non-ribosomal mRNPs, 40S, 60S, 80S and polysome. The expression of 5′tDR-GlyGCC in 40S, 60S and 80S were measured by TaqMan qRT-PCR; (**D**) compared to the scrambled control RNA group, 18 extra proteins were precipitated by both 5′tDR-GlyGCC and 5′tDR-GlnCTG in HeLa cells; (**E**) after crosslinking, the RPS21-binding RNAs were pulled down by the specific antibody. The 5′tDRs in input and RPS-binding RNAs were measured by TaqMan qRT-PCR and normalized to the total RNA amount; (**F**) both cap-dependent translation (R-luc) and IRES-dependent translation (F-luc) were normalized with LacZ activity as transfection control. The IRES-dependent translation (F-luc) were compared between wild type (WT) and *Alkbh3*$^{-/-}$ cells for all the three groups; (**G**) both 5′tDR-GlyGCC and 5′tDR-GlnCTG had statistically significant effects on the HCV IRES reporter in HeLa cells; (**H**) HeLa cells transfected with control RNA or 5′tDR-GlyGCC for 24 h were further treated with $NaAsO_2$ for 6 h, stained with annexin V and propidium iodide (PI), and analyzed by flow cytometry (*left*). The percentages of apoptotic cells (annexin V and PI double positive) were quantified (*right*); (**I**) the caspase 3 and cleaved caspase 3 in cells treated as (I) were measured by western blot analysis. Data were presented as means ± SD from three independent experiments. The reporter assays were replicated for six times for each group. *$P < 0.05$, **$P < 0.01$ compared with control. See also Supplementary Figure S6.

ery opens a potential new paradigm of tRNA demethylase which regulates cellular biological functions via induction of tDRs.

ALKBH3 has been suggested to function as a DNA-repair protein to protect the genomic integrity (21,45). Analogously to ALKBH2, ALKBH3 contains a flexible hairpin which is involved in base flipping to distinguish single-stranded substrates from double-stranded substrates (19). Our findings revealed that ALKBH3 mainly located in cytoplasm and functioned as a demethylase in tRNA. *In vitro* and *in vivo* studies showed that ALKBH3 specifically demethylated m^1A and m^3C, but not other modifications, in tRNA, which was in line with previous biochemical assay that recombinant ALKBH3 demethylated m^1A and m^3C of purified tRNA *in vitro* (46). Ueda *et al* (46) reported that ALKBH3 can demethylate m^6A of tRNA, while this effect was not observed in our present study. The exist of m^6A in mammalian tRNA is still a controversial issue (47).

Modifications of tRNA are crucial for its structural maintenance, biological functions and stability. Our data showed that ALKBH3 catalyzed m^1A and m^3C demethylation of tRNA mainly in the monosome of cytoplasm. m^1A58, which is essential to the tRNA stability (9,10), is the predominant substrate of ALKBH3 in our present study.

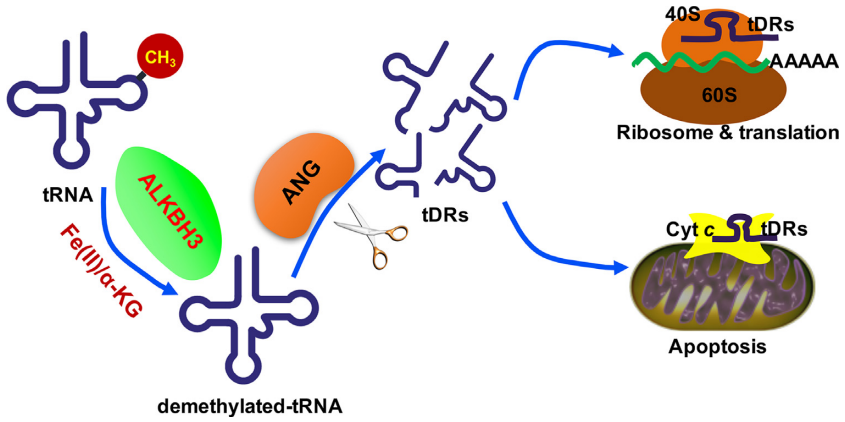

Figure 7. Proposed model of tDRs-mediated cancer progression triggered by ALKBH3. ALKBH3 catalyzed m^1A and m^3C demethylation, which increases sensitivity of tRNA to ANG cleavage, leading to the formation of tDRs. ALKBH3-generated tDRs triggers the ribosome assembly and interacts with Cyt *c* to prevent cell apoptosis.

For m^3C modification, position 32 was the most frequently modified site in cytoplasmic tRNA, as well as the position 47 in $tRNA^{Ser}$ and position 20 in $tRNA^{Met\text{-}e}$ (10,48). Demethylation of m^1A in tRNA catalyzed by ALKBH1 affected the levels of $tRNA^{iMet}$ and translation initiation (18). Although we showed that ALKBH3 had comparable demethylation activities with ALKBH1, CLIP-seq showed that $tRNA^{iMet}$ was not the target of ALKBH3. Further, neither m^1A modification nor cellular level of $tRNA^{iMet}$ was modulated by ALKBH3. In addition, ALKBH3 had no effect on tRNA-mediated translation elongation. Our data showed that 55% of ALKBH3-bound tRNAs (GluCTC, GlyGCC, HisGTG, LysCTT, AlaAGC, AlaTGC, CysGCA, LysTTT, AsnGTT, ValCAC, LeuAAG) were also the targets of ALKBH1 in HeLa cells (18). While over expression of ALKBH3 had no effect on the expression of ALKBH1 in HeLa cells (data not shown). Thus, the potential reciprocal nature of tRNA demethylation between ALKBH1 and ALKBH3 remained to be elucidated.

Existence of high-abundant tDRs was supported by increasing literatures (30,32,38,41), while biogenesis of tDRs has not been clearly illustrated. Our data indicated that ALKBH3 triggered the production of tDRs, which mainly due to its function as m^1A demethylase of tRNA. It has been reported that lack of m^1A58 impairs the hydrogen bonds from A58 to A54 and A60 in initiator $tRNA^{Met}$ of yeast, leading to the degradation of $tRNA^{Met}$ (11). Yeast strains deficient in Trm6 (or Trm61) tRNA:m^1A58-methyltransferases display a reduced level of $tRNA^{iMet}$ at elevated temperatures (49). Although there is no direct evidence about m^1A58 and tRNA stability in human cells, our present study found that ALKBH3, which acted as a tRNA demethylase, induced the generation of tDRs in both human cells and mouse tissues. Science ALKBH3-induced tDRs were mainly originated from tRNAs without m^3C modification, we hypothesized that m^1A demethylation induced by ALKBH3 can reduce the stability of tRNA, resulting in the generation of tDRs. The detailed mechanisms underlying this process need further clarification. Molecular sizes of ALKBH3-induced tDRs are similar to those induced by stresses (30–40 nt) (44), which indicated that variations of m^1A may also participate in the tDRs generation upon stress responses.

ALKBH3 had no significant effect on the expression of most its CLIP-targeted tRNA. Previous observations indicated that only a fraction of mature tRNAs are cleaved upon stress responses, causing a negligible change in the total tRNA pool (38). This might be due to that homeostasis of tRNA, which is essential for cellular functions and cell survival, is highly regulated by tRNA synthetases and related proteins (5). Inhibition of $tRNA^{GlyGCC}$, the only up-regulated tRNA in *Alkbh3*$^{-/-}$ cells, had no obvious effect on growth inhibition triggered by deletion of ALKBH3. It suggested that the biological functions of ALKBH3, as tRNA demethylase, might be related to the byproducts of tRNA rather than mature tRNA themselves. Notably, it has been reported that there was a conserved methylation in D-loop of tRNA, which can sufficiently suppress the tRNA-mediated immune stimulations in human cells (50). Whether ALKBH3 is associated to this conserved tRNA methylation and therefore modulating immune stimulations, or even mediating other tRNA modifications to trigger novel biological functions need to be further investigated.

Our data showed that tDRs were involved in ALKBH3-promoted cancer progression. This was supported by evidences that: 1) both endogenous and synthesized tDRs can trigger the cancer progression and protein synthesis. It has been reported that tRNA halves can promote the progression of breast and prostate cancers via enhancing cell proliferation (32). Besides, transfection of tDR-Gln19 up-regulated 356 proteins while only down-regulated 43 proteins, particularly increasing the translation of ribosomal and poly(A)-binding protein (51); 2) ANG, which has been reported as the RNase that responsible for tRNA cleavage in mammalian cells (38), can support the proliferation of progenitor cells after radiation damages (52).

Biological functions of tDRs and related mechanisms are far from well-illustrated. On one hand, it has been reported that tDRs suppresses the translation initiation via displacing eIF4G/eIF4A from uncapped > capped RNAs (53). On the other hand, cleavage of tRNA by ANG up-regulates the

translation of IRES-containing mRNAs such as encoding vascular endothelial growth factor (VEGF) (54) and promotes cell proliferation (32). Ueda *et al.* (46) reported that *in vitro* translation efficiency of ALKBH3-treated tRNA was higher than that of control tRNA. Our data showed that tDRs were enriched in 40/60S monosomes and interacted with ribosomal proteins such as RPS21 and RPL26. Reporter assays indicated that tDRs regulated translation processes via recruiting 40S ribosome directly. Considering that biological functions of tDRs might be cell state/type-specific (52), the inconsistent results may due to the variations of tDR types, RNA modifications and cell lines.

Our study also revealed that ALKBH3-induced tDRs interacted with Cyt *c* to regulate cell apoptosis. It was evidenced by the results that tDRs bound to Cyt *c* and suppressed stress-induced apoptosis. The tDRs-Cyt *c* complex was formed in cytoplasm when Cyt *c* was released from the mitochondria, thus preventing the formation of apoptosome and activation of caspase, resulting in the inhibition of cell apoptosis (44). Involvement of tDRs in cell apoptosis was confirmed by the observations that *Alkbh3*$^{-/-}$ cells were more sensitive to stress-induced apoptosis. Considering that tDRs can target specific signaling pathways to regulate cellular functions, the roles of tDRs in ALKBH3-triggered cancer progression need to be further studied.

Collectively, we found that ALKBH3-mediated tRNA demethylation regulates cancer progression via induction of tDRs, which can modulate the translation by regulating ribosome assembly and prevent apoptosis through binding with Cyt *c*. Our present discovery here revealed a novel relationship between tDRs generation and tRNA modifications, which will stimulate the future studies about reversible tRNA methylation on human health and diseases.

DECLARATIONS

Consent for publication

The authors confirmed that we have obtained written consent from the patient to publish the manuscript.

SUPPLEMENTARY DATA

Supplementary Data are available at NAR Online.

ACKNOWLEDGEMENTS

We thanked Prof Chuan He for data analysis and discussion, Phillip Hsu, Miss Hailing Shi, Dr Ziyang Hao and Lisheng Zhang's help for experimental skills.
Authors' contributions: Conception and design: Hongsheng Wang, Zhuojia Chen, Meijie Qi; Acquisition of data: Hongsheng Wang, Zhuojia Chen, Yingmin Wu, Zhong Zheng, Qing Dai; Analysis and interpretation of data: Guanzheng Luo, Bin Shen, Zhike Lu; Writing, review, and/or revision of the manuscript: Hongsheng Wang, Jiexin Li.

FUNDING

National Natural Science Foundation of China [81673454, 81672608, 81472470, 31801197, 81572270]; Guangdong Natural Science Funds for Distinguished Young Scholar [2014A030306025]; the Guangdong Provincial Key Laboratory of Construction Foundation [No. 2017B030314030]; Guangdong Province Key Laboratory of Malignant Tumor Epigenetics and Gene Regulation [2017B030314026]; Fundamental Research Funds for the Central Universities (Sun Yat-sen University) [16ykpy09]; China Postdoctoral Science Foundation [2018M643354]. Funding for open access charge: National Natural Science Foundation of China [81673454].
Conflict of interest statement. None declared.

REFERENCES

1. Lewis,C.J., Pan,T. and Kalsotra,A. (2017) RNA modifications and structures cooperate to guide RNA-protein interactions. *Nat. Rev. Mol. Cell Biol.*, **18**, 202–210.
2. Torres,A.G., Batlle,E. and Ribas de Pouplana,L. (2014) Role of tRNA modifications in human diseases. *Trends Mol. Med.*, **20**, 306–314.
3. Saikia,M., Fu,Y., Pavon-Eternod,M., He,C. and Pan,T. (2010) Genome-wide analysis of N1-methyl-adenosine modification in human tRNAs. *RNA*, **16**, 1317–1327.
4. Novoa,E.M., Pavon-Eternod,M., Pan,T. and Ribas de Pouplana,L. (2012) A role for tRNA modifications in genome structure and codon usage. *Cell*, **149**, 202–213.
5. Schimmel,P. (2018) The emerging complexity of the tRNA world: mammalian tRNAs beyond protein synthesis. *Nat. Rev. Mol. Cell Biol.*, **19**, 45–58.
6. Pan,T. (2018) Modifications and functional genomics of human transfer RNA. *Cell Res.*, **28**, 395–404.
7. Oerum,S., Degut,C., Barraud,P. and Tisne,C. (2017) m1A Post-Transcriptional Modification in tRNAs. *Biomolecules*, **7**, E20.
8. Roundtree,I.A., Evans,M.E., Pan,T. and He,C. (2017) Dynamic RNA Modifications in Gene Expression Regulation. *Cell*, **169**, 1187–1200.
9. Cozen,A.E., Quartley,E., Holmes,A.D., Hrabeta-Robinson,E., Phizicky,E.M. and Lowe,T.M. (2015) ARM-seq: AlkB-facilitated RNA methylation sequencing reveals a complex landscape of modified tRNA fragments. *Nat. Methods*, **12**, 879–884.
10. Clark,W.C., Evans,M.E., Dominissini,D., Zheng,G.Q. and Pan,T. (2016) tRNA base methylation identification and quantification via high-throughput sequencing. *RNA*, **22**, 1771–1784.
11. Basavappa,R. and Sigler,P.B. (1991) The 3 A crystal structure of yeast initiator tRNA: functional implications in initiator/elongator discrimination. *EMBO J.*, **10**, 3105–3111.
12. Kirchner,S. and Ignatova,Z. (2015) Emerging roles of tRNA in adaptive translation, signalling dynamics and disease. *Nat. Rev. Genet.*, **16**, 98–112.
13. Swinehart,W.E. and Jackman,J.E. (2015) Diversity in mechanism and function of tRNA methyltransferases. *RNA Biol.*, **12**, 398–411.
14. Jia,G., Fu,Y., Zhao,X., Dai,Q., Zheng,G., Yang,Y., Yi,C., Lindahl,T., Pan,T., Yang,Y.G. *et al.* (2011) N6-methyladenosine in nuclear RNA is a major substrate of the obesity-associated FTO. *Nat. Chem. Biol.*, **7**, 885–887.
15. Zheng,G., Dahl,J.A., Niu,Y., Fedorcsak,P., Huang,C.M., Li,C.J., Vagbo,C.B., Shi,Y., Wang,W.L., Song,S.H. *et al.* (2013) ALKBH5 is a mammalian RNA demethylase that impacts RNA metabolism and mouse fertility. *Mol. Cell*, **49**, 18–29.
16. Claussnitzer,M., Dankel,S.N., Kim,K.H., Quon,G., Meuleman,W., Haugen,C., Glunk,V., Sousa,I.S., Beaudry,J.L., Puviindran,V. *et al.* (2015) FTO obesity variant circuitry and adipocyte browning in humans. *N. Engl. J. Med.*, **373**, 895–907.
17. Li,Z., Weng,H., Su,R., Weng,X., Zuo,Z., Li,C., Huang,H., Nachtergaele,S., Dong,L., Hu,C. *et al.* (2017) FTO plays an oncogenic role in acute myeloid leukemia as a N6-Methyladenosine RNA demethylase. *Cancer Cell*, **31**, 127–141.
18. Liu,F., Clark,W., Luo,G., Wang,X., Fu,Y., Wei,J., Wang,X., Hao,Z., Dai,Q., Zheng,G. *et al.* (2016) ALKBH1-Mediated tRNA demethylation regulates translation. *Cell*, **167**, 1897.
19. Aas,P.A., Otterlei,M., Falnes,P.O., Vagbo,C.B., Skorpen,F., Akbari,M., Sundheim,O., Bjoras,M., Slupphaug,G., Seeberg,E. *et al.* (2003) Human and bacterial oxidative demethylases repair alkylation damage in both RNA and DNA. *Nature*, **421**, 859–863.

20. Ougland,R., Zhang,C.M., Liiv,A., Johansen,R.F., Seeberg,E., Hou,Y.M., Remme,J. and Falnes,P.O. (2004) AlkB restores the biological function of mRNA and tRNA inactivated by chemical methylation. *Mol. Cell*, **16**, 107–116.
21. Dango,S., Mosammaparast,N., Sowa,M.E., Xiong,L.J., Wu,F., Park,K., Rubin,M., Gygi,S., Harper,J.W. and Shi,Y. (2011) DNA unwinding by ASCC3 helicase is coupled to ALKBH3-dependent DNA alkylation repair and cancer cell proliferation. *Mol. Cell*, **44**, 373–384.
22. Monsen,V.T., Sundheim,O., Aas,P.A., Westbye,M.P., Sousa,M.M., Slupphaug,G. and Krokan,H.E. (2010) Divergent ss-hairpins determine double-strand versus single-strand substrate recognition of human AlkB-homologues 2 and 3. *Nucleic Acids Res.*, **38**, 6447–6455.
23. Konishi,N., Nakamura,M., Ishida,E., Shimada,K., Mitsui,E., Yoshikawa,R., Yamamoto,H. and Tsujikawa,K. (2005) High expression of a new marker PCA-1 in human prostate carcinoma. *Clin. Cancer Res.*, **11**, 5090–5097.
24. Tasaki,M., Shimada,K., Kimura,H., Tsujikawa,K. and Konishi,N. (2011) ALKBH3, a human AlkB homologue, contributes to cell survival in human non-small-cell lung cancer. *Br. J. Cancer*, **104**, 700–706.
25. Shimada,K., Fujii,T., Tsujikawa,K., Anai,S., Fujimoto,K. and Konishi,N. (2012) ALKBH3 contributes to survival and angiogenesis of human urothelial carcinoma cells through NADPH oxidase and tweak/Fn14/VEGF signals. *Clin. Cancer Res.*, **18**, 5247–5255.
26. Luo,J., Emanuele,M.J., Li,D., Creighton,C.J., Schlabach,M.R., Westbrook,T.F., Wong,K.K. and Elledge,S.J. (2009) A genome-wide RNAi screen identifies multiple synthetic lethal interactions with the Ras oncogene. *Cell*, **137**, 835–848.
27. Liu,F., Clark,W., Luo,G., Wang,X., Fu,Y., Wei,J., Wang,X., Hao,Z., Dai,Q., Zheng,G. *et al.* (2016) ALKBH1-Mediated tRNA demethylation regulates translation. *Cell*, **167**, 816–828.
28. Zheng,G.Q., Dahl,J.A., Niu,Y.M., Fedorcsak,P., Huang,C.M., Li,C.J., Vagbo,C.B., Shi,Y., Wang,W.L., Song,S.H. *et al.* (2013) ALKBH5 is a mammalian RNA demethylase that impacts RNA metabolism and mouse fertility. *Mol. Cell*, **49**, 18–29.
29. Wang,X., Zhao,B.S., Roundtree,I.A., Lu,Z., Han,D., Ma,H., Weng,X., Chen,K., Shi,H. and He,C. (2015) N(6)-methyladenosine modulates messenger RNA translation efficiency. *Cell*, **161**, 1388–1399.
30. Goodarzi,H., Liu,X., Nguyen,H.C., Zhang,S., Fish,L. and Tavazoie,S.F. (2015) Endogenous tRNA-Derived fragments suppress breast cancer progression via YBX1 displacement. *Cell*, **161**, 790–802.
31. Schuber,F. and Pinck,M. (1974) On the chemical reactivity of aminoacyl-tRNA ester bond. 2. Aminolysis by tris and diethanolamine. *Biochimie*, **56**, 391–395.
32. Honda,S., Loher,P., Shigematsu,M., Palazzo,J.P., Suzuki,R., Imoto,I., Rigoutsos,I. and Kirino,Y. (2015) Sex hormone-dependent tRNA halves enhance cell proliferation in breast and prostate cancers. *Proc. Natl. Acad. Sci. U.S.A.*, **112**, E3816–E3825.
33. Sundheim,O., Vagbo,C.B., Bjoras,M., Sousa,M.M., Talstad,V., Aas,P.A., Drablos,F., Krokan,H.E., Tainer,J.A. and Slupphaug,G. (2006) Human ABH3 structure and key residues for oxidative demethylation to reverse DNA/RNA damage. *EMBO J.*, **25**, 3389–3397.
34. Dewe,J.M., Fuller,B.L., Lentini,J.M., Kellner,S.M. and Fu,D. (2017) TRMT1-Catalyzed tRNA modifications are required for redox homeostasis to ensure proper cellular proliferation and oxidative stress survival. *Mol. Cell. Biol.*, **37**, e00214–17.
35. Yamato,I., Sho,M., Shimada,K., Hotta,K., Ueda,Y., Yasuda,S., Shigi,N., Konishi,N., Tsujikawa,K. and Nakajima,Y. (2012) PCA-1/ALKBH3 contributes to pancreatic cancer by supporting apoptotic resistance and angiogenesis. *Cancer Res.*, **72**, 4829–4839.
36. Goodarzi,H., Nguyen,H.C.B., Zhang,S., Dill,B.D., Molina,H. and Tavazoie,S.F. (2016) Modulated expression of specific tRNAs drives gene expression and cancer progression. *Cell*, **165**, 1416–1427.
37. Zhang,X., Cozen,A.E., Liu,Y., Chen,Q. and Lowe,T.M. (2016) Small RNA Modifications: Integral to function and disease. *Trends Mol. Med.*, **22**, 1025–1034.
38. Thompson,D.M. and Parker,R. (2009) Stressing out over tRNA cleavage. *Cell*, **138**, 215–219.
39. Yamasaki,S., Ivanov,P., Hu,G.F. and Anderson,P. (2009) Angiogenin cleaves tRNA and promotes stress-induced translational repression. *J. Cell Biol.*, **185**, 35–42.
40. Schaefer,M., Pollex,T., Hanna,K., Tuorto,F., Meusburger,M., Helm,M. and Lyko,F. (2010) RNA methylation by Dnmt2 protects transfer RNAs against stress-induced cleavage. *Genes Dev.*, **24**, 1590–1595.
41. Sharma,U., Conine,C.C., Shea,J.M., Boskovic,A., Derr,A.G., Bing,X.Y., Belleannee,C., Kucukural,A., Serra,R.W., Sun,F. *et al.* (2016) Biogenesis and function of tRNA fragments during sperm maturation and fertilization in mammals. *Science*, **351**, 391–396.
42. Kumar,P., Kuscu,C. and Dutta,A. (2016) Biogenesis and function of transfer RNA-Related Fragments (tRFs). *Trends Biochem. Sci.*, **41**, 679–689.
43. Hertz,M.I., Landry,D.M., Willis,A.E., Luo,G. and Thompson,S.R. (2013) Ribosomal protein S25 dependency reveals a common mechanism for diverse internal ribosome entry sites and ribosome shunting. *Mol. Cell. Biol.*, **33**, 1016–1026.
44. Saikia,M., Jobava,R., Parisien,M., Putnam,A., Krokowski,D., Gao,X.-H., Guan,B.-J., Yuan,Y., Jankowsky,E., Feng,Z. *et al.* (2014) Angiogenin-cleaved tRNA halves interact with cytochrome c, protecting cells from apoptosis during osmotic stress. *Mol. Cell. Biol.*, **34**, 2450–2463.
45. Zheng,G., Fu,Y. and He,C. (2014) Nucleic acid oxidation in DNA damage repair and epigenetics. *Chem. Rev.*, **114**, 4602–4620.
46. Ueda,Y., Ooshio,I., Fusamae,Y., Kitae,K., Kawaguchi,M., Jingushi,K., Hase,H., Harada,K., Hirata,K. and Tsujikawa,K. (2017) AlkB homolog 3-mediated tRNA demethylation promotes protein synthesis in cancer cells. *Sci. Rep.*, **7**, 42271.
47. Randerath,K., MacKinnon,S.K. and Randerath,E. (1971) An investigation of the minor base composition of transfer RNA in normal human brain and malignant brain tumors. *FEBS Lett.*, **15**, 81–84.
48. Olson,M.V., Page,G.S., Sentenac,A., Piper,P.W., Worthington,M., Weiss,R.B. and Hall,B.D. (1981) Only one of two closely related yeast suppressor tRNA genes contains an intervening sequence. *Nature*, **291**, 464–469.
49. Kadaba,S., Krueger,A., Trice,T., Krecic,A.M., Hinnebusch,A.G. and Anderson,J. (2004) Nuclear surveillance and degradation of hypomodified initiator tRNAMet in S. cerevisiae. *Genes Dev.*, **18**, 1227–1240.
50. Gehrig,S., Eberle,M.E., Botschen,F., Rimbach,K., Eberle,F., Eigenbrod,T., Kaiser,S., Holmes,W.M., Erdmann,V.A., Sprinzl,M. *et al.* (2012) Identification of modifications in microbial, native tRNA that suppress immunostimulatory activity. *J. Exp. Med.*, **209**, 225–233.
51. Keam,S.P., Sobala,A., Ten Have,S. and Hutvagner,G. (2017) tRNA-Derived RNA fragments associate with human multisynthetase complex (MSC) and modulate ribosomal protein translation. *J. Proteome Res.*, **16**, 413–420.
52. Goncalves,K.A., Silberstein,L., Li,S., Severe,N., Hu,M.G., Yang,H., Scadden,D.T. and Hu,G.-F. (2016) Angiogenin promotes hematopoietic regeneration by dichotomously regulating quiescence of stem and progenitor cells. *Cell*, **166**, 894–906.
53. Ivanov,P., Emara,M.M., Villen,J., Gygi,S.P. and Anderson,P. (2011) Angiogenin-induced tRNA fragments inhibit translation initiation. *Mol. Cell*, **43**, 613–623.
54. Holcik,M. and Sonenberg,N. (2005) Translational control in stress and apoptosis. *Nat. Rev. Mol. Cell Biol.*, **6**, 318–327.